



ELSEVIER

New Astronomy 1 (2002) 000–000

New Astronomy

www.elsevier.com/locate/newast

A rotating differential accelerometer for testing the equivalence principle in space: results from laboratory tests of a ground prototype

A.M. Nobili^{a,*}, D. Bramanti^a, G.L. Comandi^a, R. Toncelli^a, E. Polacco^b

^a*Space Mechanics Group, Department of Mathematics, University of Pisa, I-56127 Pisa, Italy*

^b*Department of Physics, University of Pisa, and INFN, I-56127 Pisa, Italy*

Received 19 August 2002; accepted 1 November 2002

Communicated by F. Melchiorri

Abstract

We have proposed to test the equivalence principle (EP) in low Earth orbit with a rapidly rotating differential accelerometer (made of weakly coupled concentric test cylinders) whose rotation provides high frequency signal modulation and avoids severe limitations otherwise due to operation at room temperature [PhRvD 63 (2001) 101101]. Although the accelerometer has been conceived for best performance in absence of weight, we have designed, built and tested a variant of it at 1-g. Here we report the results of measurements performed so far. Losses measured with the full system in operation yield a quality factor only four times smaller than the value required for the proposed high accuracy EP test in space. Unstable whirl motions, which are known to arise in the system and might be a matter of concern, are found to grow as slowly as predicted and can be stabilized. The capacitance differential read-out (the mechanical parts, electronics and software for data analysis) is in all similar to what is needed in the space experiment. In the instrument described here the coupling of the test masses is 24 000 times stiffer than in the one proposed for flight, which makes it 24 000 times less sensitive to differential displacements. With this stiffness it should detect test masses separations of $1.5 \cdot 10^{-2} \mu\text{m}$, while so far we have achieved only $1.5 \mu\text{m}$, because of large perturbations—due to the motor, the ball bearings, the non-perfect verticality of the system—all of which, however, are absent in space. The effects of these perturbations should be reduced by 100 times in order to perform a better demonstration. Further instrument improvements are underway to fill this gap and also to reduce its stiffness, thus increasing its significance as a prototype of the space experiment.

© 2002 Elsevier Science B.V. All rights reserved.

PACS: 04.80.Cc; 07.10.-h; 06.30.Bp; 07.87.+v

Keywords: Gravitation; Relativity; Instrumentation: detectors; Methods: laboratory; Methods: data analysis

*Corresponding author.

E-mail addresses: nobili@dm.unipi.it (A.M. Nobili),
bramanti@mail.dm.unipi.it (D. Bramanti),
comandi@mail.dm.unipi.it (G.L. Comandi),
toncelli@mail.dm.unipi.it (R. Toncelli),
polacco@mail.dm.unipi.it (E. Polacco).

1384-1076/02/\$ – see front matter © 2002 Elsevier Science B.V. All rights reserved.

doi:10.1016/S1384-1076(02)00233-6

1. Introduction

The equivalence principle (EP) stated by Galileo, reformulated by Newton and reexamined by Einstein to become the founding principle of General Relativity, can be tested from its most direct conse-

quence: the universality of free fall (UFF), whereby all bodies fall with the same acceleration regardless of their mass and composition ($\eta = \Delta a/a = 0$). The most accurate EP experiments have been carried out on the ground with test bodies suspended on a torsion balance, finding no violation to about 10^{-13} (Adelberger et al., 1990; Su et al., 1994; Baeßler et al., 1999). (See Note added in proof.) Test bodies in low Earth orbit are subject to a driving gravitational (and inertial) acceleration much stronger than on torsion balances on the ground, by about three orders of magnitude. Moreover, the absence of weight is ideal in small force experiments. As a consequence, space missions can potentially improve by several orders of magnitude the current sensitivity in EP tests. Three such experiments are being considered, and the goals are: 10^{-15} for the French μ SCOPE (MICROSCOPE Website:

http://www.cnes.fr/activites/activites/connaissance/physique/microsatellite/1sommaire_microsatellite.htm and

<http://www.onera.fr/dmph-en/accelerometre>; Touboul et al., 2001), 10^{-17} for the Italian “GALILEO GALILEI” (GG) (“GALILEO GALILEI” (GG), Phase A Report, 1998; Nobili et al., 1999; “GALILEO GALILEI” (GG) Website: <http://eotvos.dm.unipi.it/nobili>; Nobili et al., 2001), 10^{-18} for the American STEP (Worden, 1978; STEP Satellite Test of the Equivalence Principle, 1993; STEP Satellite Test of the Equivalence Principle, 1996; Step Website: <http://einstein.stanford.edu/STEP>) [however, STEP studies within the European Space Agency are consistent with a goal of 10^{-17} (STEP Satellite Test of the Equivalence Principle, 1993; STEP Satellite Test of the Equivalence Principle, 1996)]. μ SCOPE and GG are room temperature experiments, STEP is cryogenic at very low temperature.

In all the proposed space experiments the test bodies are hollow cylinders one inside the other, with their centers of mass as close as possible for classical differential effects (such as tides) to be reduced. However, in spite of the different arrangement of the test bodies needed in space, the main features of the ground apparatus which have so far provided the best sensitivity should be retained. The most relevant of such features is the differential nature of the torsion balance, which makes it ideally

insensitive to common mode effects. Its implementation at the end of the 19th century (Eötvös et al., 1922) has provided a major improvement, by about three orders of magnitude, over previous pendulum tests of the EP. However, Eötvös tested the universality of free fall in the field of the Earth, therefore looking for a constant (DC) anomalous acceleration in the North–South direction of the plane of the horizon. Another major improvement (by about three more orders of magnitude) was made possible in the 1960s and 1970s (Roll et al., 1964; Braginsky and Panov, 1972) when a torsion balance was used to search for a deviation from UFF in the field of the Sun, in which case the diurnal rotation of the Earth itself provides a 24-h modulation of the expected signal. Further improvements on the torsion balance, including its rotation faster than the diurnal rotation of the Earth (at ≈ 1 h period) and consequent modulation of the signal at higher frequency, have provided the most sensitive tests so far (Adelberger et al., 1990; Su et al., 1994; Baeßler et al., 1999)

It seems therefore appropriate, for an EP experiment in space, that the instrument be designed as a rotating differential accelerometer made of concentric test cylinders, thus leading naturally to a spacecraft of cylindrical symmetry too, and co-rotating with the test cylinders. If the axis of symmetry is the axis of maximum moment of inertia, one-axis rotation provides (passive) spacecraft attitude stabilization. This is how the GG space experiment for testing the EP in the field of the Earth has been designed: the concentric test cylinders spin around the symmetry axis at a rather high frequency (2 Hz with respect to the center of the Earth) and are sensitive to differential effects in the plane perpendicular to the spin/symmetry axis. A cylindrical spacecraft encloses, in a nested configuration, a cylindrical cage with the test cylinders inside, and is stabilized by rotation around the symmetry axis. As shown in Fig. 1, an EP violation in the field of the Earth would generate a signal of constant amplitude (for zero orbital eccentricity) whose direction is always pointing to the center of the Earth, hence changing orientation with the orbital period of the satellite. The read-out, also rotating with the system, will therefore modulate an EP violation signal at its spin frequency.

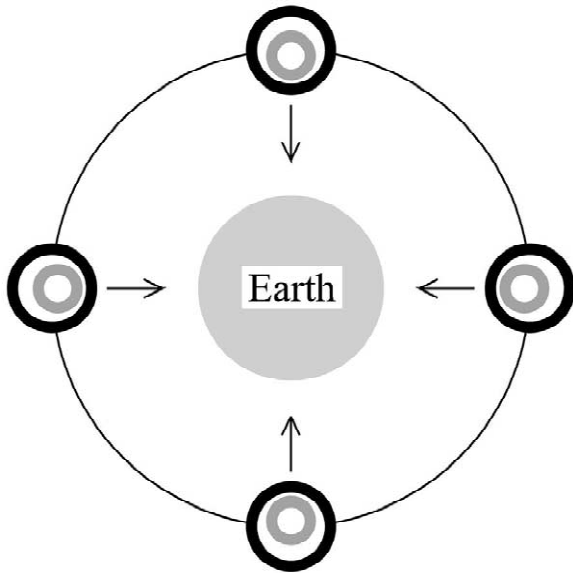


Fig. 1. Section across the spin/symmetry axis of the GG outer and inner test cylinders (of different composition) as they orbit around the Earth inside a co-rotating, passively stabilized spacecraft (not shown). The centers of mass of the test cylinders are shown to be displaced towards the center of the Earth as in the case of a violation of the equivalence principle in the field of the Earth (indicated by the arrows). The signal is modulated at the spin frequency of the system (2 Hz with respect to the center of the Earth). The figure is not to scale (taken from Nobili et al., 2001).

We have designed and built a differential, rotating accelerometer similar to the one proposed for the GG space experiment. It is a full scale prototype devoted to testing the main features of the proposed instrument, in spite of the fact that the local acceleration of gravity is about eight orders of magnitude bigger than the largest disturbances the accelerometer would be subject to in space (due to the residual air drag and to solar radiation pressure). Here we describe the ground apparatus, show how it is operated and report the results obtained from measurement data so far. To conclude, we discuss the relevance of these results in view of the GG target sensitivity.

2. Design of the apparatus

A schematic view of the apparatus is given in Fig. 2, where a section through the spin/symmetry axis

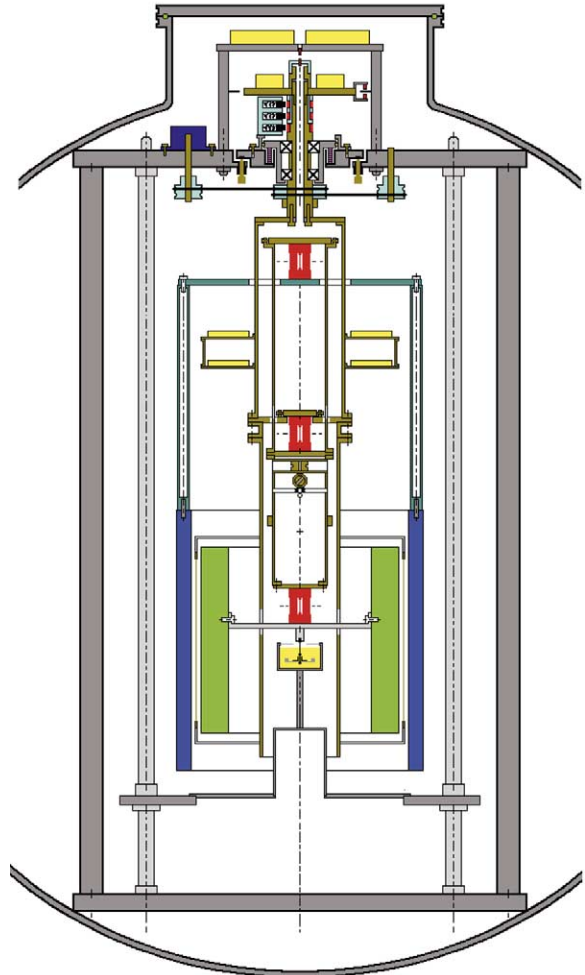


Fig. 2. Section through the spin axis of the differential accelerometer inside the vacuum chamber (drawing to scale; inner diameter of vacuum chamber 1 m; see text for a description of its parts).

of the accelerometer is shown (enclosed by the vacuum chamber). (The color version of Fig. 2 is available in the article published on the World Wide Web.) Fig. 3 shows a picture of the accelerometer mounted inside the chamber. In Fig. 2 the chamber and the frame (not rotating) on which the whole rotor is mounted are drawn in gray. The test cylinders are drawn in green (the inner one) and blue (the outer one). On the top of the frame (at its center) is a shaft turning inside ball bearings (sketched as “x” in the section of Fig. 2) to which rotation is transmitted from the motor by means of O-rings on pulleys. This

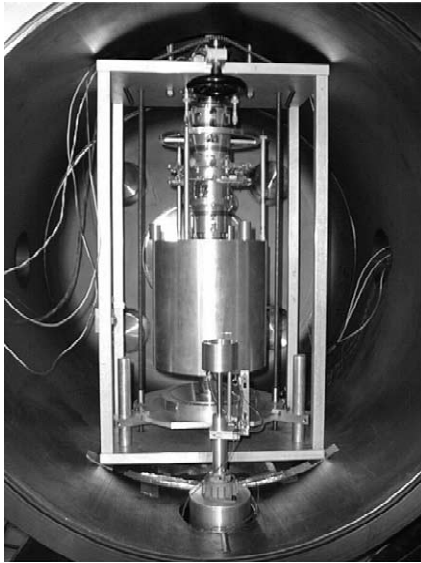


Fig. 3. The rotating differential accelerometer mounted inside the vacuum chamber (in the basement of the LABEN laboratories in Florence).

shaft holds the suspension tube, which therefore rotates with the shaft. Inside the suspension tube is the coupling arm (also a tube) suspended at its midpoint from the suspension tube by means of a laminar suspension (drawn in red; see picture in Fig. 4). The two test cylinders are suspended from the two ends of the coupling arm (the outer one from the top, the inner one from the bottom) by two more laminar suspensions (all three suspensions are manufactured to be equal; they are all drawn in red in Fig. 2). Being metallic, they also ensure passive electrostatic discharging of the test masses. Fig. 3 shows three light vertical bars and a horizontal ring used to connect the outer test cylinder to its suspension at the top of the coupling arm. The suspensions have the property of being soft in both the X and Y directions in the plane perpendicular to the symmetry/vertical axis, while at the same time being strong enough in the vertical direction in order to withstand local gravity. In this way the test cylinders—in spite of being concentric—are in fact suspended like in an ordinary beam balance, but with the beam of the balance (the coupling arm) in the vertical direction rather than in the horizontal one. The central suspension (connecting the midpoint of the beam to the

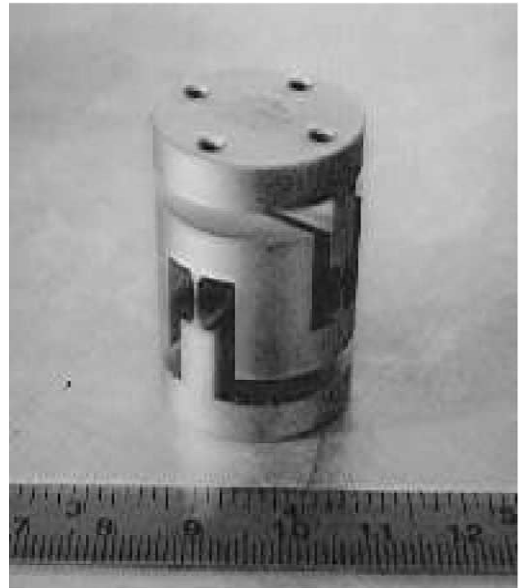


Fig. 4. One of the three laminar suspensions used in the accelerometer (sketched in red in Fig. 2). They are carved out of a solid bar of CuBe by electroerosion in 3D and properly treated for high mechanical quality.

suspension tube) is therefore the one which carries the whole weight of this balance, mostly due to the test cylinders themselves (10 kg each).

The read-out consists of two pairs of capacitance plates located halfway in between the test cylinders and connected to the suspension tube by means of an insulating frame (see picture in Fig. 5 and section in Fig. 2, in which they appear as vertical lines in between the test cylinders). They maintain the cylindrical symmetry of the system, forming two capacitance bridges in the X and Y directions of the plane perpendicular to the symmetry axis (the plane of sensitivity of the instrument). The two annular dishes (in yellow) mounted around the upper half of the suspension tube contain the two capacitance bridge circuits, their preamplifiers, the signal demodulators, the A/D (analog-to-digital) converters and the driver of the optical emitter, which is located at the very top of the rotating shaft (in order to transmit the demodulated signal from the rotor to the non-rotating frame and then outside of the vacuum chamber). In the upper part of the shaft, above the ball bearings, are the rotating contacts for power transmission to the electronics of the rotor and a dish with a circuit



Fig. 5. The four capacitance plates (with their insulating frames) forming the two capacitance bridges of the read-out. They are mounted halfway in between the concentric test cylinders to read their relative displacements (see section in Fig. 2).

for stabilizing this power. To this dish is also attached an optical device which provides a reference signal for the phase of the rotor. The passive damper is shown under the lowest laminar suspension, and is not rotating (see Section 4).

A differential force acting between the test cylinders in any direction in the horizontal plane of the laboratory will incline the balance beam—pivoted at its midpoint—with respect to the vertical, thus giving rise to a relative displacement of the centers of mass of the cylinders in the direction of the force. The resulting mechanical displacement will unbalance the capacitance bridges, thus allowing it to be transformed into an electric voltage signal. If the whole system (test cylinders plus read-out) rotates around the vertical shaft, the signal is modulated at the rotation frequency, just as in the GG space experiment (Fig. 1). In case of an EP violation in the field of the Earth, two test cylinders of different composition should show (after transformation to the non-rotating reference frame) a constant, relative displacement in the North–South direction of the horizontal plane. Instead, checking for violation in the field of the Sun requires to detect a (smaller) relative displacement vector in the same plane following the Sun in its daily motion with respect to the Earth fixed laboratory where the test bodies are located.

The instrument is therefore a rotating differential

accelerometer sensitive in the horizontal plane. Its differential character comes from two features. The first is that the test cylinders are mechanically coupled so as to be sensitive to differential accelerations acting between them because of the geometry of their mounting. The second is that the read-out too is differential: were all plates mounted exactly halfway in between the test cylinders (same clear gap on either side), it would be totally insensitive to common mode forces (i.e., to forces causing a displacement of both test cylinders together with respect to the capacitance plates). For a non-zero off-centering of the plates between the cylinders, the read-out is anyway less sensitive to common mode displacements than it is to differential ones, by a factor which is the ratio of the off-centering to the average gap: the better the plates are centered, the less sensitive is the read-out to common mode forces, the more suitable it is for EP testing. The sensitivity of the test cylinders to differential accelerations depends on the softness of the laminar suspensions and the balance of arms and masses in their coupled mounting. Soft suspensions and good balancing are needed, providing long natural periods of differential oscillations of the test cylinders with respect to one another. The longer the natural periods of differential oscillations, the larger the mechanical displacements of the test cylinders in response to differential accelerations, the stronger the output voltage signal. Soft suspensions and good balancing are also needed in order to reduce the residual differential fraction of forces which are common mode by their nature but do in fact produce also a differential effect on the test cylinders due to the inevitable imperfections in their mounting and balancing. Ideally, a common mode force should be perfectly rejected by the system, leaving no differential residual. By comparison, the test cylinders of the μ SCOPE accelerometer (also based on capacitance sensing) are controlled with respect to the same silica frame but are not coupled, neither by the suspensions (each cylinder has its own electrostatic suspension) nor by the read-out (the differential data of interest are obtained as the difference of the individual readings of the capacitance sensors of each test cylinder (MICROSCOPE Website: http://www.cnes.fr/activites/activites/connaissance/physique/microsatellite/1sommaire_microsatellite).

htm and [http://www.onera.fr/dmph-en/accelerometre; Touboul et al., 2001, Fig. 1](http://www.onera.fr/dmph-en/accelerometre;Touboul%20et%20al.,%202001,%20Fig.%201)).

Ordinary beam balances are known to be ideal instruments for extremely effective common mode rejection (rejection factors of 10^{-8} – 10^{-9} can be reached at 1-g). Also in the accelerometer designed for space (see Fig. 6 and its caption; the color version of Fig. 6 is available in the article published on the World Wide Web) the test cylinders are coupled like in a beam balance—with the plane of sensitivity perpendicular to the beam as in Fig. 2—and have a differential capacitance read-out. The geometry of the space accelerometer is perfectly symmetric, which is possible in the absence of weight because the direction of the beam is not the direction of a force many orders of magnitude larger than any force acting in the sensitivity plane perpendicular to it, as it is the case with the vertical balance of Fig. 2 because of the local acceleration of gravity.

In this case the advantage of the coupling of the test cylinders is retained in spite of a lack of symmetry in their suspension arms: the center of mass of the inner cylinder is very close to its suspension point, while the center of mass of the outer one is much farther from its own (see Fig. 2). This asymmetry is a consequence of the special character of the vertical direction when operating at 1-g and it is an inevitable change from the perfect symmetry of the space design.

It is desirable that the spin rate be high, so as to get a correspondingly high frequency modulation of the signal and consequent reduction of $1/f$ mechanical and electronic noise. It is also desirable for the mechanical coupling between the test cylinders to be weak (long natural differential period T_{diff}), for them to be sensitive to differential forces like the one which would result from an EP violation, because the relative displacement due to a differential force increases as T_{diff}^2 . This means that typically the

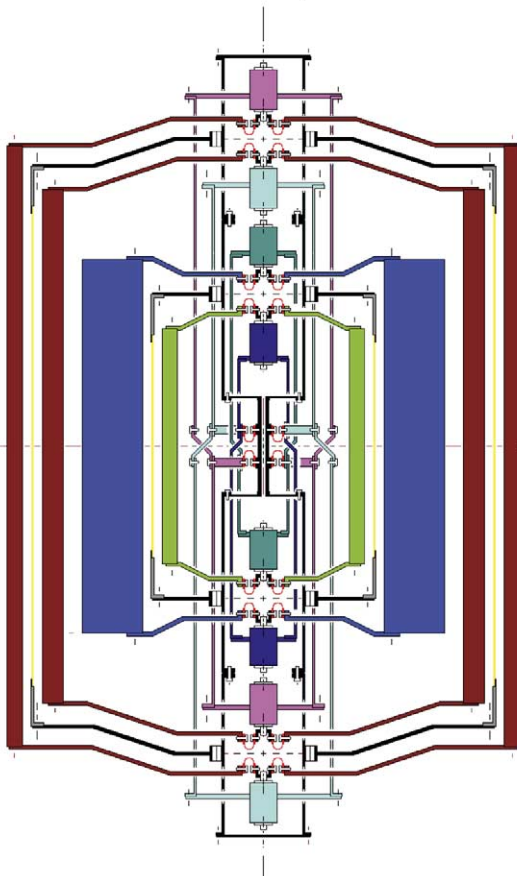


Fig. 6. Section through the spin axis of the differential accelerometers of the proposed GG mission for testing the equivalence principle in low Earth orbit. There are four test cylinders (10 kg each), one inside the other, all centered at the same point (nominally, the center of mass of the spacecraft) forming two differential accelerometers: the inner one for EP testing (cylinders of different composition; shown in green and blue respectively) and the outer one for zero check (cylinders made of the same material; both shown in brown). In each accelerometer the two test cylinders are coupled to form a beam balance by being suspended at their top and bottom from the two ends of a coupling arm made of two concentric tubes (each tube suspends one test cylinder at each end, which makes it asymmetric top/down; however, the two of them together form a symmetric coupling). All four tubes (two for each coupling arm) are suspended at their midpoints from the same suspension shaft (the longest vertical tube in figure). In all cases the suspensions are U-shape (or \cap -shape) thin strips (shown in red), to be carved out of a solid piece of CuBe. At each connection there are three of them, at 120° from one another (the planar section in figure shows two for explanatory purposes only). There are capacitance plates (connected to the suspension shaft) for the read-out of differential displacements in between each pair of test cylinders (shown as yellow lines in section). The eight small cylinders drawn along the symmetry axis are inchworms for the fine adjustment of the lengths of the coupling arms in order to center each test mass on the center of mass of the spacecraft. The whole system is symmetric around the spin axis as well as top/down. The two accelerometers are both centered at the center of mass of the spacecraft in order to reduce common mode tidal effects and improve the reliability of the zero check.

system spins at a frequency higher than the natural frequency for differential oscillations of the test cylinders, in which case it is known that the spinning bodies do reduce any original offset vector between their centers of mass (fixed in the rotating system) inevitably due to imperfections in construction and mounting (see e.g. Den Hartog, 1985; Crandall, 1995; Genta, 1993). In simple terms, a weakly coupled and fast spinning rotor is an approximation to an ideal unconstrained rotor whose center of mass would have zero offset from the rotation axis.

The natural period T_{diff} for differential oscillations of the test cylinders, one with respect to the other, in the vertical beam balance arrangement of Fig. 2 (in the presence of both local gravity and mechanical coupling) can be written as:

$$T_{\text{diff}} \approx \frac{2\pi}{\sqrt{\left(\frac{3K}{m} + \frac{g \Delta l}{2l}\right)}} \quad (1)$$

with m the mass of the test cylinder, g the local acceleration of gravity, $2l$ the length of the coupling arm (with a difference $\Delta l > 0$ between its lower and upper half respectively) and K the coupling constant (note that, for lateral flexures, K is lower than the elastic constant of the laminar suspensions shown in Fig. 4 and Fig. 2 by a factor given by the ratio, squared, of the length of the laminar suspension itself to the length l of the arm—“lever effect”). In Eq. (1) the ratio $\Delta l/l$ accounts for both the balance of arms and masses ($\Delta m/m$) attached to the beam. The validity of Eq. (1) is confirmed by numerical simulations and measurements, and shows well the relevance of gravity. If $\Delta l > 0$, gravity acts as a positive spring, thus increasing the stiffness of the coupling, i.e. reducing the length of T_{diff} . Instead, if $\Delta l < 0$, gravity acts as a negative spring and the ratio $\Delta l/l$ (indeed, $\Delta l/l$ and/or $\Delta m/m$) can be adjusted so as to reduce the denominator of Eq. (1) whereby increasing the value of T_{diff} . We have verified this, obtaining differential periods of up to about 90 s, although so far the accelerometer has been operated with differential periods around 10 s.

Natural differential oscillations in the X and Y directions as detected by the capacitance read-out are shown in Fig. 7 (zero spin rate, differential periods of 11 s). When the rotor spins at 3 Hz the differential

displacements between the test cylinders measured by the (rotating) capacitance bridges show the same natural periods, in addition to the expected rotation frequency (see Fig. 8). At zero spin the decreasing amplitude of oscillations allows the quality factor Q of the system to be measured, yielding an average value of 510. The dominant losses are due to the laminar suspensions of the rotor as deformed at the low natural differential frequencies, and for large oscillation amplitudes (up to 1 mm). Q measurements for the laminar suspensions alone—before assembling of the accelerometer—when set in horizontal oscillations at higher frequency (5 Hz) and similar oscillation amplitudes, have been performed (in vacuum), yielding Q values of 2000 (“GALILEO GALILEI” (GG), Phase A Report, 1998, Section 3.4; Nobili et al., 2000). Better (higher) Q values are expected at higher frequencies and for smaller oscillation amplitudes. However, once rotating, the suspensions are deformed at the frequency of spin and losses occur at this frequency, which is higher than the differential frequency, and should therefore result in higher Q 's (see Section 5).

Besides the natural frequency for differential oscillations the accelerometer system of Fig. 2 has two additional natural frequencies, one slightly below and one slightly above 1 Hz. The first can be viewed as the pendular frequency (common mode) of the whole system; the second one as due to the inner test cylinder being suspended close to its center of mass and having a non-zero moment of inertia with respect to the symmetry axis (if the inner mass is modeled as a point mass this frequency disappears). The predicted theoretical values of these natural frequencies have been confirmed by experimental measurements. In order to reach the spin rates of interest (above 1 Hz), the system must cross all these natural frequencies, and when passing the two nearby ones it can undergo large resonant disturbances. It has been suggested (Luo, 2000) that the system be simplified by substituting the laminar suspension of the inner test cylinder (the bottom one of the three sketched in Fig. 2; see also Fig. 4) with a solid brass cylinder of the same external dimensions. By simple readjustments of arms and masses we have set up the system for routine measurements with the natural period for differential oscillations close to 8 s and the pendular frequency slightly

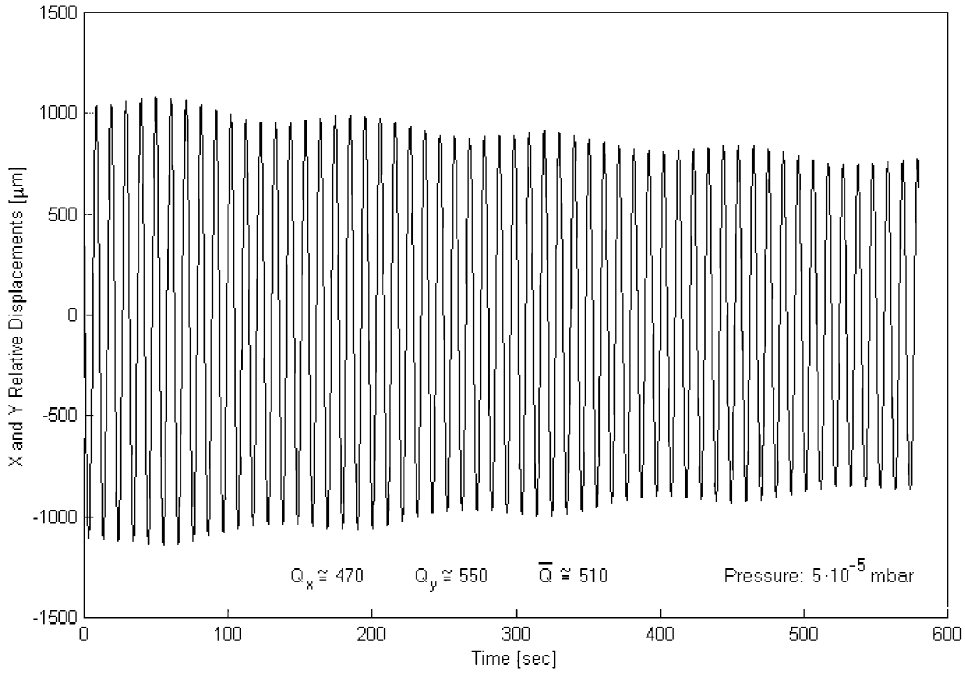


Fig. 7. Relative displacements, in the X and Y directions of the sensitivity plane, between the centers of mass of the test cylinders at zero spin rate. The natural periods of differential oscillations at 11 s are apparent. The amplitudes of these oscillations are slowly decreasing with time, yielding a quality factor of about 510 (taken from Nobili et al., 2000).

below 1 Hz. These two values were predicted theoretically and confirmed by measurements. Q measurements at variable residual pressure in the vacuum chamber are reported in Section 5. It is worth noting that in this arrangement the relevant whirl frequency of the test cylinders is split into two: a forward one, increasing with the spin rate, instead of remaining constant (as shown in Figs. 7 and 8) and a backward one. The reason is the following. A differential force acting between the test cylinders in their vertical beam balance arrangement causes a relative displacement of their centers of mass by inclining the coupling arm of the balance pivoted at its midpoint. In this case, if weakly suspended one at each end of the arm, the test cylinders keep spinning around their axes. However, if the inner test cylinder is rigidly connected to the end of the arm, the inclination of the arm forces it to spin along the arm itself, describing a whirl cone, while the angular momentum of the body would tend to conserve its vertical direction. The result is a stiffer or softer suspension of the inner test cylinder, depending on

the sense of rotation and—since the two are coupled—also a period of their whirl motions shorter or longer than that of the natural oscillations, depending on whether whirl motion is in the same sense as the rotation or in the opposite one (see Section 5). The whirl period relevant to the sensitivity of the accelerometer is the shorter one, corresponding to a stiffer coupling.

Spinning bodies are subject to gyroscopic effects, whereby they move not in the direction of the applied force but along the component of the external torque perpendicular to the spin axis. In a ground laboratory the gyroscopic effect for a body of mass m , angular momentum \vec{L} and center of mass suspended with an arm \vec{l} is due to the torque generated by the local gravity and to the angular velocity $\vec{\omega}_{\oplus}$ of the Earth’s diurnal rotation around its axis:

$$\left(\frac{d\vec{L}}{dt}\right)_{\text{lab}} = (\vec{\Omega}_g - \vec{\omega}_{\oplus}) \times \vec{L} \tag{2}$$

$$\left(\vec{\Omega}_g = -\frac{mgl}{L}, \vec{l} \times m\vec{g} = \vec{\Omega}_g \times \vec{L}\right)$$

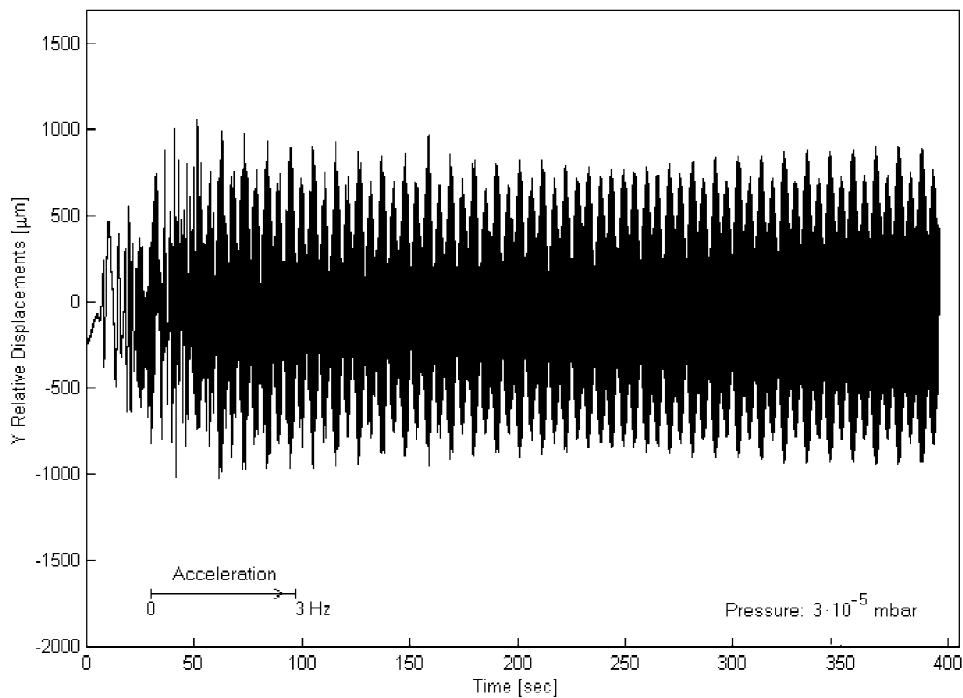


Fig. 8. Relative displacements (for the Y direction only, in the rotating reference frame) obtained with the same instrument as in Fig. 7 but having brought it to a rotation rate of 3 Hz. The natural differential oscillation at about 11 s period (the same as at zero spin) is apparent, as it is the faster rotation frequency of the system at 3 Hz.

Gravity makes the body precess around the local vertical (unless the center of mass lies exactly on the vertical itself), while the non-inertial nature of the laboratory reference frame (because of its diurnal rotation with the Earth) makes it precess around the Earth's rotation vector; the suspensions produce a restoring force towards the vertical. Equilibrium is reached in the North–South direction, the only direction along which the acting torques can balance each other. The test cylinders of Fig. 2 undergo different gyroscopic effects, resulting in a net relative displacement in the North–South direction. Its calculation shows a constant displacement at any given spin rate, and a linear increase with it, reaching several μm at a few Hz; if the laminar suspension of the inner test cylinder is substituted by a rigid connection the differential gyroscopic effect increases by about a factor of 10 (see measurements of gyroscopic effect in Section 5). In both cases it is in the same direction as the effect of an EP violation in the gravitational field of the Earth, and much larger. Instead, a relative displacement due to an EP viola-

tion in the field of the Sun would show up as an additional vector following the daily motion of the Sun (the gyroscopic constant displacement can be subtracted away during data analysis or compensated by properly changing the verticality of the suspension shaft in the North–South direction).

For this reason the rotating differential accelerometer of Figs. 2 and 3 can be used as a prototype test instrument of the one proposed for space and for testing the equivalence principle in the field of the Sun, but cannot be used for testing the equivalence principle in the field of the Earth. It is worth stressing that the gyroscopic effect would not affect the space instrument (“GALILEO GALILEI” (GG), Phase A Report, 1998, Section 2.1.2). Unlike what happens in a ground laboratory, the angular momentum vector of the rotor is almost fixed in space, undergoing only a slow precession (around the orbit normal) due to the fact that the spin axis is not exactly normal to the orbit plane and the moment of inertia with respect to the spin axis is the dominant one (“GALILEO GALILEI” (GG), Phase A Report,

1998, Eq. (2.11)) (the effect is similar to the luni-solar precession of the Earth's axis around the normal to the ecliptic). The system is symmetrical and the test cylinders are suspended from their center of mass and symmetrically with respect to it (see Fig. 6). The resulting gyroscopic effects are found to be totally negligible ("GALILEO GALILEI" (GG), Phase A Report, 1998, Section 2.1.2; Comandi, 1999, Section 3.17).

3. Adjustments and settings of the apparatus

Various adjustments can be performed for the rotating differential accelerometer to operate as it is designed to. An inclination of the (rotating) coupling arm, about its midpoint, by a non-zero (constant) angle from the vertical, gives rise to a constant relative displacement of the test cylinders fixed in the rotating frame. It is therefore detected by the (rotating) read-out as a constant offset from zero (in X and Y), which provides the driving signal for this adjustment. In order to reduce this offset the position of the top suspension (the one of the outer test cylinder; see Fig. 2) can be adjusted so as to be as much as possible in line with the other two suspensions at the center and the bottom. This is the coarsest adjustment. Then, on the coupling arm, close to (just below) the central suspension, are mounted two small masses (5 g each) that can be displaced across the arm's axis in the X and Y directions in order to reduce the corresponding offsets, and therefore the inclination of the arm. For yet a finer adjustment there are two additional smaller masses (0.5 g each), also movable in X and Y .

However, a constant offset in the X and Y measurements of the relative displacements between the centers of mass of the test cylinders as performed by the rotating capacitance bridges may also be due to the bridge capacitances being out of balance at zero mechanical displacement; which would require the variable capacitances in each bridge to be adjusted, and no change in the inclination of the coupling arm. In order to separate the two effects, and operate the right adjustment, we perform these measurements by spinning the rotor at a frequency first below and then above the natural one for differential oscillations of the test cylinders. If the offsets are due to the

inclination of the coupling arm, i.e. to the test cylinders not being suspended along the same axis, it is known that that they should decrease when spinning above the natural frequency (see e.g. Den Hartog, 1985; Crandall, 1995; Genta, 1993). Once a non-zero inclination of the coupling arm has been ruled out, we can proceed to reduce the offsets of the measurements by adjusting the variable capacitances. A few iterations of this procedure may be necessary.

Around the lower half of the coupling arm is mounted a small solid ring (see section in Fig. 2), movable in the vertical direction. A change in its vertical position, by changing the mass distribution of the beam balance, will change the natural period of the differential oscillations (see discussion on Eq. (1)). Being symmetrical around the arm, the position of the ring does not affect its inclination. From an operational viewpoint, this is the easiest way to change and adjust the differential period of the test cylinders.

In the conceptual design of the differential accelerometer it is very important that the suspension shaft (the tube enclosing the coupling arm, held by a shaft turning inside ball bearings, to which rotation from the motor is transmitted by means of O-rings on pulleys; see Fig. 2) be aligned with the local vertical. In the case of a non-zero inclination of the suspension tube from the local vertical—due to the shaft not being mounted perfectly vertical in the laboratory reference frame—there will be a non-zero lateral deformation of the central suspension which suspends the beam balance (see Fig. 2), and a consequent relative displacement of the test cylinders. The displacement is fixed in the laboratory (non-rotating) frame along the direction identified by the misalignment of the shaft and is modulated by the rotating capacitance bridges at their spin frequency. The X and Y bridge measurements are transformed into the X_{nr} and Y_{nr} relative displacements in the non-rotating frame (see Section 4) where the coordinates of the fixed displacement indicate the direction of the deflection of the suspension shaft. They provide the driving signal for this adjustment, which is performed by means of three vertical micrometric screws (at 120° from one another) which control the inclination of the top plane of the frame around the shaft (see Fig. 3), hence also its verticality. The micrometric screws are

differential and allow both coarse and fine adjustments. A still finer adjustment of the verticality of the suspension shaft is performed by means of three (vertical) piezoelectric actuators (PTZs, also at 120° from one another) perpendicular to the horizontal plane at the top of the rotor, on which it rests. They allow finer adjustments of the verticality of the shaft than micrometric screws can do, and moreover they can be remotely controlled from outside the vacuum chamber. In addition, if the central suspension which carries the weight of the whole system is not centered on the rotation axis, the centrifugal force will compress the same PZTs at the frequency of spin. Their three signals are acquired by means of a National Instruments card and allow us to adjust the position of the central suspension on the rotation axis by means of three micrometric screws mounted horizontally around it, so as to reduce the PZTs signals as much as possible.

As the system spins the suspensions are deformed at the spin frequency and the relevant loss factors (inverse of quality factor Q) are those of the mechanical suspensions at the spin frequency. The effects of such dissipation are unstable forward whirl motions whose frequencies are close to the natural frequencies of the system. The destabilizing forces which generate the whirl motions are equal to the passive spring forces divided by the Q . The magnitude of the forces is the same in the stationary and in the rotating frame; only their frequencies change. The forces required to achieve neutral equilibrium are equal and opposite to the destabilizing forces. They never exceed the passive spring forces as long as Q is larger than 1. For large Q s the destabilizing forces, as well as the active ones required for stabilization, are much smaller than the passive spring forces. This also means that the instabilities to be damped grow very slowly. The negative Q which determines the growth of the whirl motions is equal (with the opposite sign) to the Q of the suspensions at the frequency of spin (Genta, 1993; Crandall and Nobili, 1997; Nobili et al., 1999).

In the rotating accelerometer of Fig. 2 whirl motions can be stabilized either passively (by providing sufficient non-rotating damping) or actively, by means of small capacitance sensors/actuators which must be controlled to counteract the destabilizing forces which generate the whirl motions.

In the GG space experiment, where there are no non-rotating parts (no motor is needed once the spacecraft is set in rotation at the nominal spin rate) whirl motions can only be actively controlled (Nobili et al., 1999; “GALILEO GALILEI” (GG), Phase A Report, 1998, Chapter 6). In the differential accelerometer of Fig. 2 a passive, non-rotating damper, made of a very light disk with little radial blades immersed in oil for vacuum, is mounted on the inner test cylinder, below its suspension from the coupling arm (it is shown in yellow and gray in Fig. 2, but only its base is visible in Fig. 3). It stabilizes the whirl motion at the natural differential frequency of the test cylinders, as measurements show (see Section 5). The passive damper is also equipped with a mechanism mounted in the vacuum chamber outside the accelerometer itself (it is clearly visible in Fig. 3 in front of the accelerometer) that can be activated from outside the chamber in order to run the system with or without damping of whirl motion and to measure (when off) the whirl growth rate, which provides the Q of the system at the spin frequency (Section 5). We can also use this on/off mechanism during testing of the active damper. The active damper (not shown in Figs. 2 and 3) is made by eight small capacitance plates facing the outer test cylinder (one layer of four sensors and one of four actuators, the two pairs of sensors forming the two halves of two capacitance bridges in the two coordinates of the horizontal plane). The electronics of these bridges is essentially the same as that of the bridges of the main sensors (Section 4, Fig. 9) except for the fact that here smaller capacitances and less good sensitivity are needed. The signals from these two bridges drive the four (high) voltages for the four actuators.

4. Read-out and data acquisition

The relative mechanical displacements of the test cylinders in the X and Y directions of the plane perpendicular to the spin axis are read by two capacitance bridges, rotating with the system, whose four sensing plates (Fig. 5) are located in between the test cylinders with a clear gap of 5 mm on either side. The electronic circuit of each bridge is sketched in Fig. 9. The smallest fractional capacitance unbal-

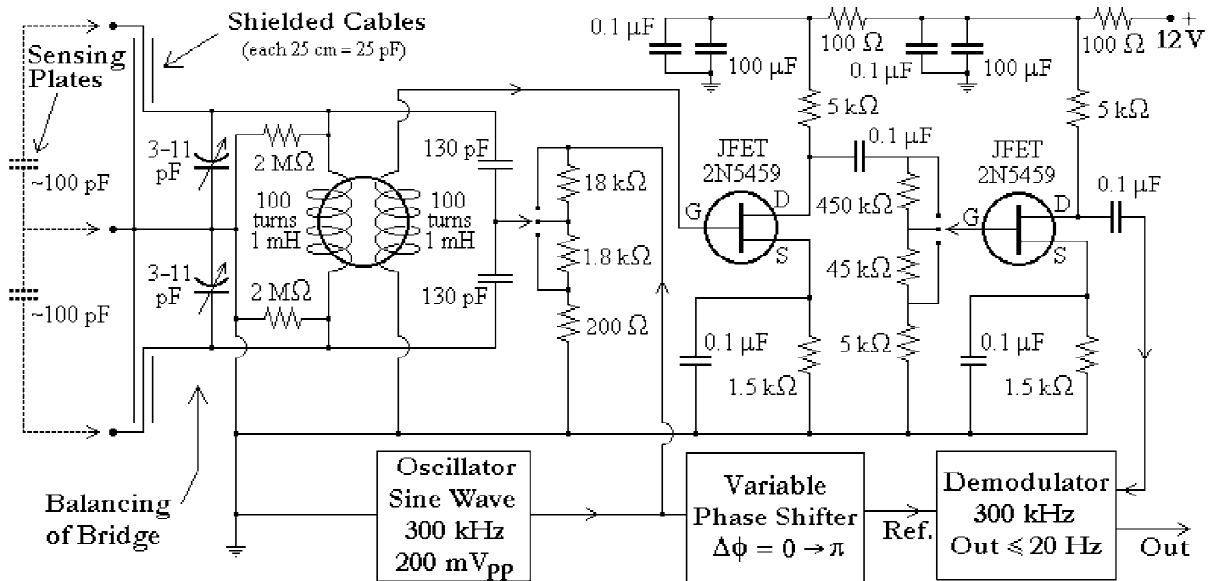


Fig. 9. The capacitance bridge sensor circuits used in the accelerometer of Figs. 2 and 3 for the read-out of the relative displacements of the test cylinders.

ance that the circuit was sensitive to in bench tests corresponds to mechanical displacements of 5 picometer in 1 s of integration time (“GALILEO GALILEI” (GG), Phase A Report, 1998, Section 2.1.3). A voltage signal of high frequency is applied to the bridge in order to shift the signal of interest to a high frequency band with reduced $1/f$ noise. Since the capacitance bridges rotate with the accelerometer, power and data transfer must be ensured between the rotating and the non-rotating frame. For power transfer we use rotating contacts. The high frequency bridge measurements are first demodulated and then converted from analog to digital to be optically transferred outside the vacuum chamber. The (rotating) electronics which is needed to perform these tasks, as well as the electronics of the bridges, is located on an annular dish mounted around the suspension tube (Figs. 2 and 3).

In order to be able to transform the relative displacements as measured by the bridges in the rotating frame of the rotor to the non-spinning reference frame of the laboratory, we need to know, in correspondence of each data point, also the phase angle of the rotor. For this purpose a simple optical device has been mounted at the top of the rotor which provides a reference signal with the rotor

phase information. A microprocessor outside the chamber takes care of combining the reference signal with the X and Y measurements and of providing the resulting combined data in RS232 data format for computer acquisition (through a serial port) as a binary file which is then transformed into a text file for data analysis. The reference signal is also acquired, independently of the capacitance bridges data, by another computer (through a National Instruments card) for independent checks of the spin rate of the system and for various other tests to ensure that the data combination procedure has been performed correctly.

The capacitance bridges are calibrated by displacing the outer test cylinder with respect to the inner one by a known amount (by means of a micrometric screw mounted on the frame for this purpose only; not shown in Fig. 3) and recording the voltage signal read by the capacitance sensors. Displacements are applied in both X and Y directions and linearity checks of the calibration curve are performed in both cases.

The electric zero of the capacitance bridges is first set at its nominal value, by setting the value of the variable capacitance of the circuit (Fig. 9). More accurate checks are performed with the system in

rotation, first below and then above the natural frequency of differential oscillations of the test cylinders, as discussed in Section 4.

Mechanical balancing should be achieved to ensure that the capacitance plates of the bridges be located halfway in between the outer surface of the inner test cylinder and the inner surface of the outer one, a configuration which provides the best sensitivity to differential displacements. The capacitance plates shown in Fig. 5 (two for each one of the two bridges in the X and Y directions), are rigidly connected (via an insulating frame) to the suspension tube (see Fig. 2). The linear dimensions of the frame are dictated by the linear dimensions of the test cylinders (outer radius of inner cylinder and inner radius of the outer one), which are chosen on the basis of the desired gap between the two. Since all parts are precisely manufactured according to the

design (their dimensions are checked a posteriori to less than $1\ \mu\text{m}$ with a 3D measuring machine equipped with a contact point sensor) it is possible to design and manufacture the insulating frames of the plates (see Fig. 5) so that they provide a configuration as close as possible to the nominal one corresponding to perfect mechanical balancing. This procedure has provided considerable improvement with respect to a previous set up in which all parts of the frame were manufactured, mounted and adjusted independently.

5. Results from measurement data

In this Section we report the results obtained during several months of operation of the rotating differential accelerometer as outlined above, with

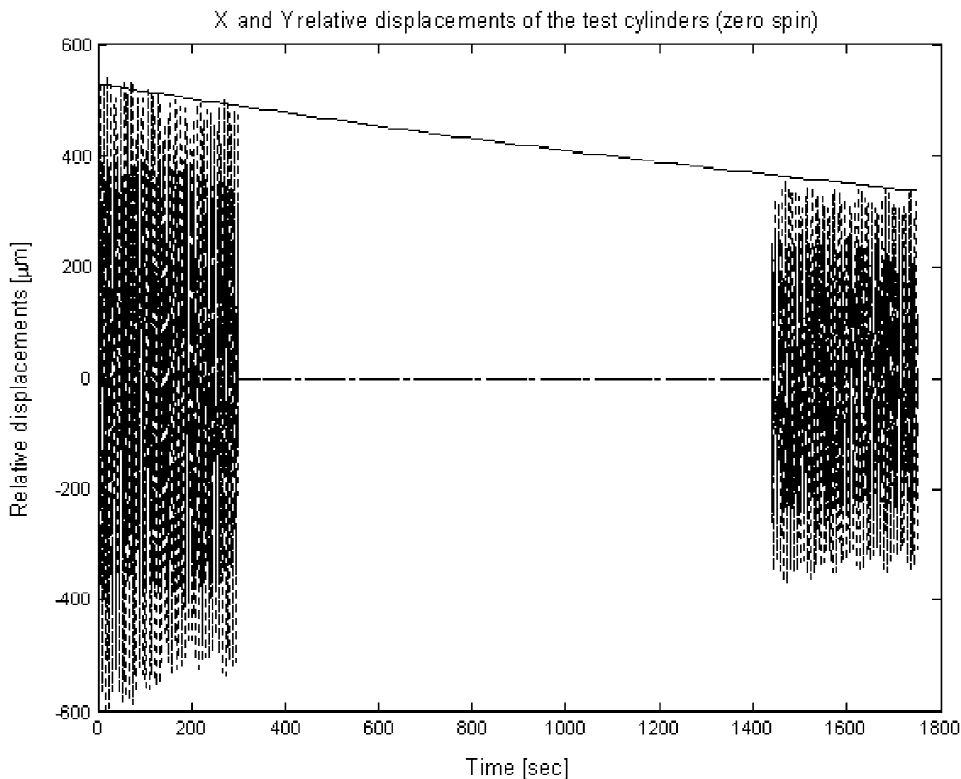


Fig. 10. Relative displacements, in the X and Y directions of the sensitivity plane, between the centers of mass of the test cylinders at zero spin rate. The natural periods of differential oscillations are of about 8 s. The amplitudes of these oscillations are slowly decreasing with time; data sets taken at subsequent times—under no changes in the system—yield a quality factor of about 1590. Residual air pressure during this measurement is of $2 \cdot 10^{-5}$ mbar.

only two relevant natural frequencies. The results concern the quality factor of the system (at the natural differential frequency and at the spin frequency), the differential gyroscopic effect, the growth rate of whirl motion and the stability in time of the differential displacement vector between the test cylinders.

Fig. 10 shows the differential oscillations of the test cylinders in the X and Y directions (at about 8 s; zero spin rate). The slow decay in the oscillation amplitudes yields a Q value of 1590. This value has been obtained in vacuum with a residual air pressure of $2 \cdot 10^{-5}$ mbar.

By performing Q measurements at different pressures it was possible to establish that residual air in between the test cylinders gives rise to dissipation. Losses due to air friction linearly decrease with pressure until they remain constant and no longer depend on the decreasing pressure (below a few 10^{-5} mbar). Fig. 11 shows well this phenomenon and indicates that, as long as the system is operated at sufficiently low pressure, losses depend on the laminar suspensions only. Note that $Q = 1590$, as

from Fig. 10 for oscillations at ≈ 8 s, is about three times better than the Q value previously obtained (at 11 s; see Fig. 7).

It is very important to check that gyroscopic effects are as theoretically expected. For this reason numerous measurements have been performed, at various spin frequencies both in clockwise and counterclockwise rotation. Relative gyroscopic displacements of the test cylinders are expected in the North–South direction of the horizontal plane of the laboratory (towards South for counterclockwise rotation, towards North for clockwise rotation), and the amount of the displacement should increase linearly with the spin rate. Measurements reported in Fig. 12 (with a fit to a straight line) show agreement with the theoretical predictions. Each data point in the plot has been obtained from the raw data of the capacitance bridges (in the rotating reference frame) acquired as discussed in Section 4, by coordinate transformation to the non-spinning laboratory frame (see Section 4) and after averaging out of short periodic variations.

The fit is good, but the amount of the displace-

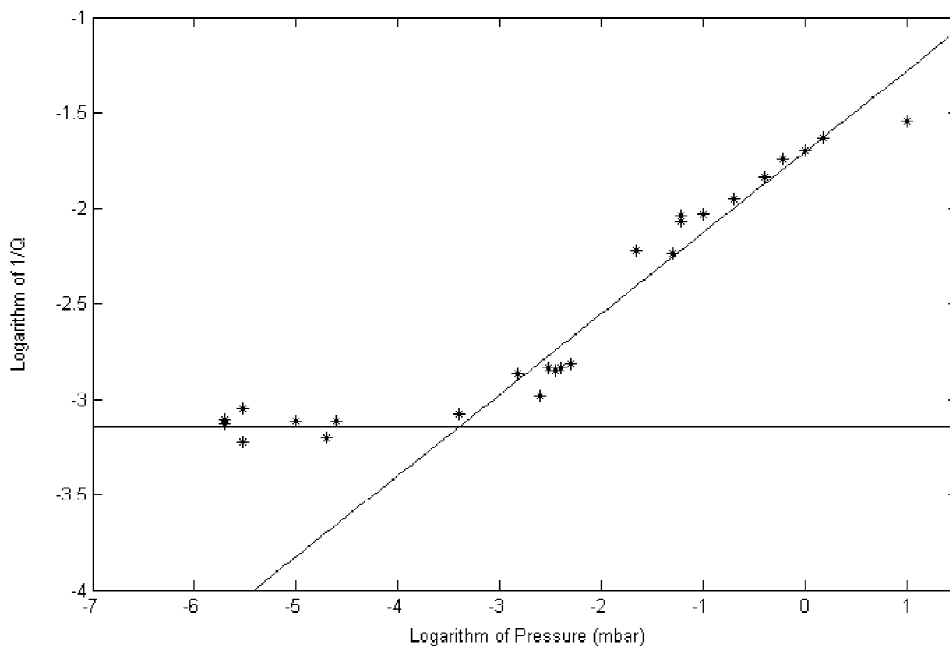


Fig. 11. Log–Log plot of the $1/Q$ value of the natural differential oscillations (≈ 8 s period), at zero spin rate, as function of the residual air pressure in the chamber with linear best fits to the two sets of data, above and below 10^{-3} mbar. Each point refers to a separate run. For pressures greater than about 10^{-3} mbar the value of Q decreases as pressure increases. For lower pressures the value of Q reaches about 1590 and is then independent of pressure since it is the maximum value allowed by losses in the laminar suspensions.

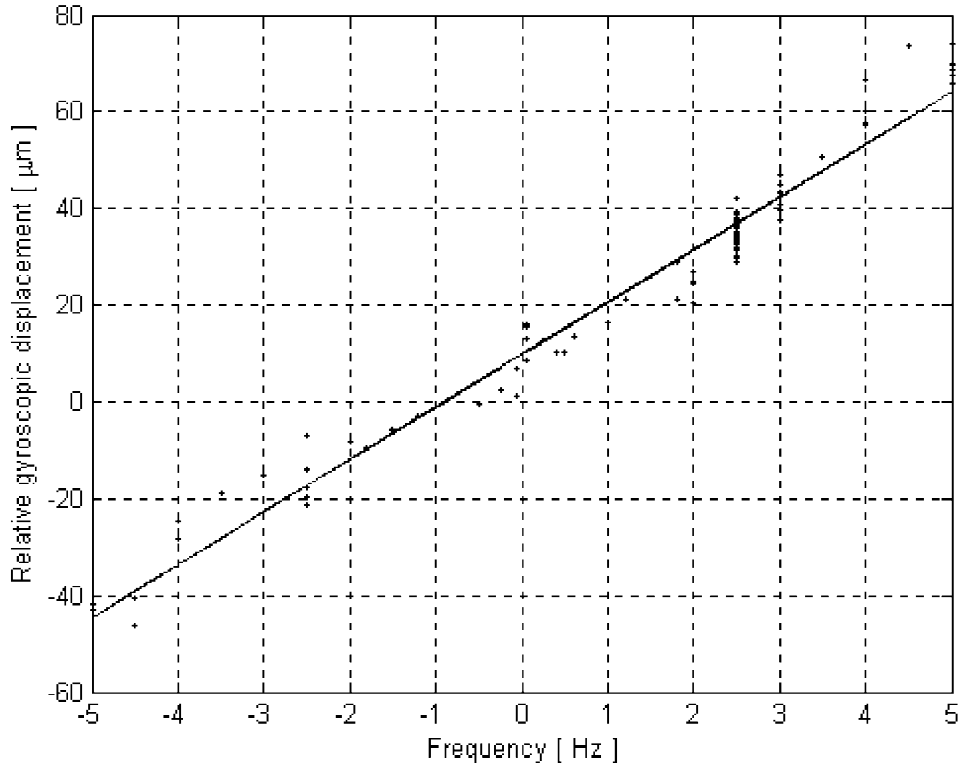


Fig. 12. Relative displacements (crosses) of the test cylinders, fixed in the horizontal plane of the laboratory, as function of the spin frequency and the sense of rotation, with linear fit to a straight line (on the frequency axis, counterclockwise spin frequencies are indicated as positive, clockwise ones as negative). The linear increase with the spin rate and the change of sign can be ascribed to the gyroscopic effect. The offset at zero spin is due to the inclination of the suspension shaft from the vertical.

ment is higher than originally expected. The disagreement is explained once the effect is calculated taking into account that the laminar suspension of the inner test cylinder (at the bottom end of the coupling arm) had been replaced by a solid brass cylinder connecting it to the lower half of the coupling arm, suspended from the central laminar suspension. At any given spin rate the relative gyroscopic displacement of the test cylinders, plus any original deviation of the suspension shaft from the local vertical, produce a relative displacement vector fixed in the non-spinning reference frame of the laboratory. Any smaller, slowly changing differential effect must be detected as an additional relative vector moving around this fixed displacement. The smaller the deviation from a fixed displacement, the more sensitive is the accelerometer to low frequency differential effects (such as the one due to an EP violation in the field of the Sun, with a 24-h period). The fixed

displacement can be subtracted away during data analysis; however, once the nominal spin rate has been chosen, the verticality of the suspension shaft (in the laboratory frame) can be adjusted (as discussed in Section 3) so as to compensate for the gyroscopic effect at the working spin rate.

Although whirl motions at the natural frequencies can be damped, it is very important to know how rapidly they grow, i.e. how strong are the destabilizing forces (due to losses in the suspensions at the spin frequency) which need to be counteracted. It is apparent that, the slower is the growth rate of whirl motions, the easier it is to stabilize the system, the smaller are the perturbations caused by the required damping on the signal of interest (Nobili et al., 1999).

We have therefore performed long runs (up to several hours) with the accelerometer spinning at a few Hz and no damping applied (neither passive nor

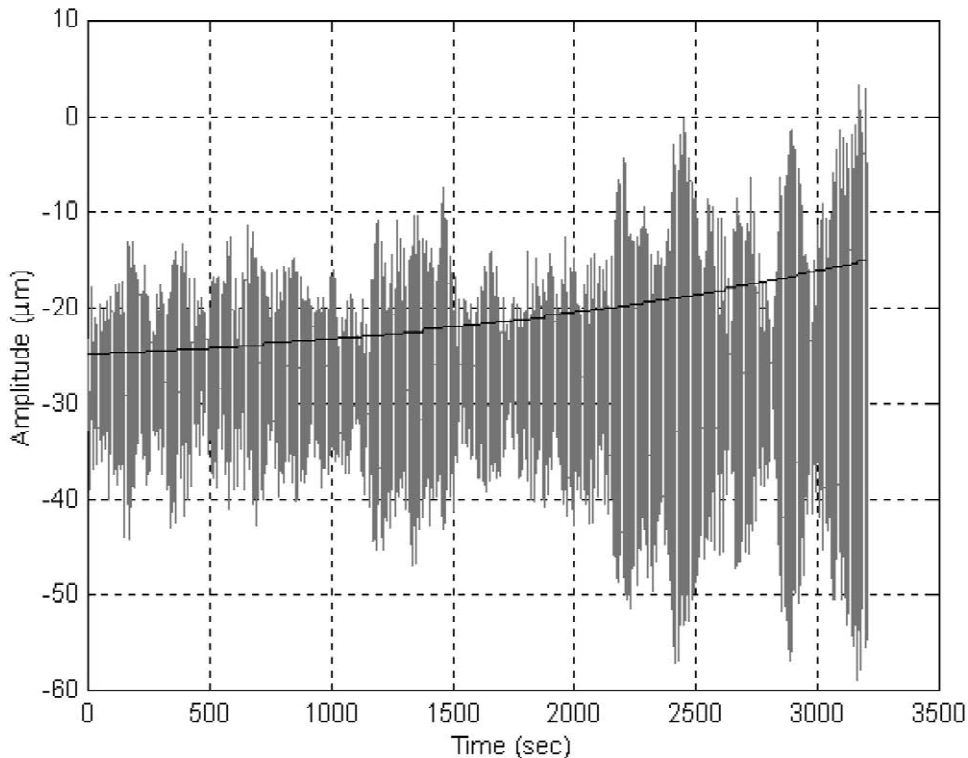


Fig. 13. Amplitude of the relative displacements between the test cylinders once transformed in the non-rotating plane of the laboratory (at a spin rate of 2.5 Hz). The growth in oscillation amplitude is due to an undamped whirl motion at 0.74 Hz. Its growth is represented by the exponential curve, and is due to losses in the system (at the spin frequency) corresponding to a Q value of 4900.

active). Pressure in the chamber was low enough to rule out any dissipation due to residual air (see Fig. 11) and data from the capacitance bridge sensors were taken continuously in order to monitor the growth of oscillation amplitudes (whirl motions at the natural frequencies in the laboratory frame show up as oscillations close to the spin frequency in the reading of the X and Y relative displacements of the test cylinders by the rotating capacitance bridges). We have runs of 3.5 h in which no appreciable growth in the oscillation amplitude could be detected. A shorter run is shown in Fig. 13 (at a spin rate of 2.5 Hz), in which the oscillation amplitude of an undamped whirl motion at 0.74 Hz shows a growth corresponding to a (negative) Q of 4900, which is therefore (with the positive sign) the quality factor of the system at the frequency of spin. We can compare it to a Q of about 2000 measured for the laminar suspension only (Fig. 4), by setting it in oscillation at 5 Hz and monitoring the decay with

time of the oscillation amplitude. The measurement was performed for horizontal oscillation only, for the measured Q not to be affected by local gravity; the amplitude of the oscillations was much larger (“GALILEO GALILEI” (GG), Phase A Report, 1998, Section 3.4; Nobili et al., 2000).

The relevant physical quantity which remains to be measured is the stability in time of the relative position of the test cylinders in the horizontal plane of the laboratory, non-rotating, frame after short periodic effects have been filtered out. Fig. 14 gives an example. It shows, for a run at 2.5 Hz, the relative displacements of the test cylinders in the horizontal plane of the laboratory after coordinate transformation of the capacitance bridges measurements from the rotating reference frame to the non-rotating one. The curve gives the relative motion as time goes by, roughly represented with color: from blue at the beginning to green at the end of the run. The motion occurs away from the origin (zero relative displacements).

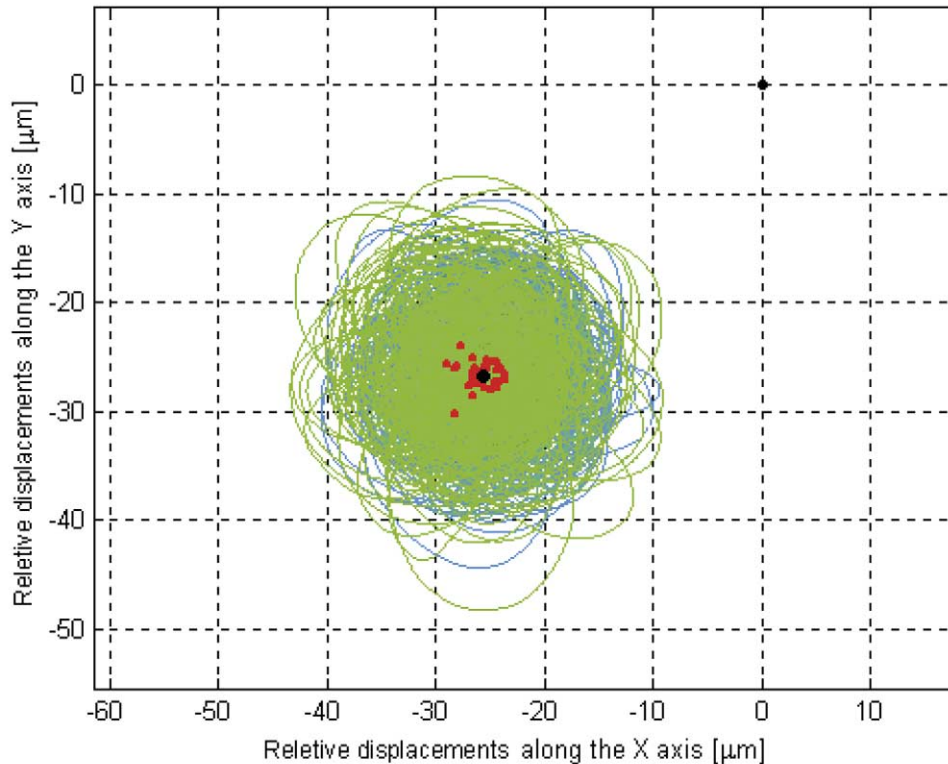


Fig. 14. Relative displacements of the test cylinders in the horizontal (non-rotating) plane of the laboratory with the accelerometer spinning at 2.5 Hz (counterclockwise). The position of relative equilibrium (the black dot at the middle of the figure) is displaced towards South (in this plot North is at 45° , i.e. in the $+X$, $+Y$ direction) because of the gyroscopic effect and short periodic relative motions occur around it. Average over the differential whirl period gives the red dots from whose average the black dot is obtained, thus defining the relative equilibrium vector for this data set (lasting 660 s) of a run lasting about 1 h.

ment), around an equilibrium position vector (vector head plotted as a black dot) dominated by the gyroscopic effect (towards the South of the laboratory plane in this case because the accelerometer spins counterclockwise). This equilibrium vector is computed as the average of the vectors (whose heads are plotted as red dots), which are obtained from the average over the whirl period (3.5 s at 2.5 Hz spin frequency; the decrease from the value of the differential period observed at zero spin, shown in Fig. 10, is due to the inner test cylinder being rigidly connected to the bottom end of the coupling arm, as pointed out in Section 2). By performing a continuous run of measurements, with the accelerometer spinning at a given spin rate, we can compute, for various data sets of the same run, the coordinates of the black dot, and check its stability in time. The more stable it is, the better is the instrument sen-

sitivity. The best result obtained so far is a stability of $1.5 \mu\text{m}$ in 1 h (at a spin rate of 2.5 Hz).

It is worth stressing that the large perturbations that give rise to these displacements are not unexpected: they are due to the motor, to the ball bearings, to the non-perfect verticality of the system, all causes that will be absent in the space experiment. Firstly, because in the space experiment there is no motor (once the spacecraft has been brought to the desired rotation speed by small tangential jets, these jets can be completely turned off). Then, because there are no bearings, since the whole spacecraft rotates with all its parts at the same rotational speed. Then, because the direction of the rotation axis is not critical, since there is no 1-g force of gravity to withstand. Other perturbations, such as terrain tilts and microseisms, are by far more relevant for the ground prototype than it is residual

vibration noise inside the spacecraft. The only perturbations on the ground that have a corresponding perturbation in space, in addition to thermal noise, are the slow whirling instabilities which, according to the measurements reported above, do not appear to be the limiting factor to the observed stability of the relative position of the test cylinders. There is therefore no physical reason to expect that the same perturbations, or other perturbations as large as these, will act on the planned space experiment.

6. Concluding remarks

We have built a rotating differential accelerometer, at room temperature, with fast spinning test cylinders (10 kg each) suspended like in a vertical beam balance so as to be weakly coupled in the horizontal plane. In spite of the need to sustain its weight, the coupled system is very sensitive to differential forces acting between the test cylinders in the horizontal plane; in addition, the read-out is made of capacitance bridges which read the relative displacements of the test cylinders directly (instead of deriving them as the difference of their individual displacements). This makes the accelerometer well suited for detecting tiny differential effects; by comparison, the proposed μ SCOPE accelerometer (also at room temperature and based on capacitance sensors) is not inherently differential because each test cylinder has an independent suspension and sensing system (although both cylinders are controlled with respect to the same silica frame) (MICROSCOPE Website: http://www.cnes.fr/activites/activites/connaissance/physique/microsatellite/1sommaire_microsatellite.htm and <http://www.onera.fr/dmph-en/accelerometre>; Touboul et al., 2001, Fig. 1). The quality factor of the system has been measured at the spin frequency, as well as at the low frequency of differential oscillations (when at zero spin rate). The results are consistent with those obtained in previous measurements for losses in the mechanical suspensions alone (Nobili et al., 1999, 2000). Unstable whirl motions which are predicted because of such losses have been found to grow very slowly, according to the Q values, and therefore very small forces are needed to stabilize them (see Nobili et al., 1999 for the relevance of this issue). Gyroscopic effects have

been measured and shown to be in agreement with their theoretical prediction. Finally, it is found that the stability of the present prototype is such that, at 2.5 Hz spin rate and 3.5 s period of whirl, the 10 kg mass test cylinders remain within 1.5 μm from each other for 1 h.

These results are relevant for the space variant of this instrument, proposed for the GG space mission, in several respects. Losses in the system and whirl motions are in agreement with predictions, giving us confidence in the theoretical analysis and numerical simulations of the GG dynamical system carried out so far (“GALILEO GALILEI” (GG), Phase A Report, 1998, Chapter 6). The relevant quality factor, as measured with the accelerometer in full operation, is only a factor four smaller than the quality factor required in the GG error budget for its target sensitivity in EP testing of 10^{-17} : 4900 instead of the 20 000 value required (“GALILEO GALILEI” (GG), Phase A Report, 1998, Section 2.2.7). (Note that we have measured $Q = 19\,000$ for a low stiffness CuBe suspension, suitable for use in space, when set in horizontal oscillation at 5 Hz (Nobili et al., 1999, 2000). The read-out (mechanical parts and electronics), data acquisition and data analysis (including the need for accurate coordinate transformation from the rotating to the non-rotating frame of reference) are of direct relevance to the space instrument and its operation. The stability observed in the relative position of the test cylinders can be compared with the GG requirement as follows. The spin rate is almost the same (the nominal spin rate of GG is 2 Hz), but the test cylinders in space can be coupled much more weakly than on the ground, thanks to the absence of weight. We have 3.5 s whirl period in our recent measurement runs and expect to be able to reach 540 s in space (as in the GG mission baseline at Phase A study level (“GALILEO GALILEI” (GG), Phase A Report, 1998), the relative displacement of the test cylinders in response to differential forces being proportional to the square of the differential period (and inversely proportional to the stiffness of the suspensions). An EP violation signal would have a well defined signature (frequency and phase), in both the ground and the space experiment, so the relevant sensitivity of the instrument has to be assessed for this target signal. In space (Fig. 1) the signal is a relative displacement vector of fixed length pointing to the Earth and

therefore changing direction with the orbital period of the spacecraft. On the ground it is a fixed displacement in the North–South direction if the source mass under consideration is the Earth; it is a displacement vector whose length and direction change with the daily (and also annual) motion of the Sun if the Sun is the source mass. In all cases, the rotation of the instrument provides higher frequency modulation of the displacement vector. For GG to reach its target sensitivity, the relative displacement of the test cylinders in the satellite-to-Earth direction, modulated at the high frequency of spin and then transformed into a constant signal in the non-rotating reference frame, should not exceed $\Delta r_{\text{GG}} = 6.2 \cdot 10^{-11}$ cm (“GALILEO GALILEI” (GG), Phase A Report, 1998, Section 2.1.1). Bench tests have demonstrated that the sensitivity of our read-out electronics is of $5 \cdot 10^{-10}$ cm in 1 s of integration time (“GALILEO GALILEI” (GG), Phase A Report, 1998, Section 2.1.3), allowing us to detect the target displacement Δr_{GG} of the space experiment in about 100 s. So, the observed 1.5 μm separation between the centers of mass of the test cylinders is due to the ground perturbations mentioned at the end of the previous section, while the read-out electronics could detect much smaller displacements. The ground prototype, whose measurements of the relative displacements of the test cylinders are reported here, is stiffer than the one proposed for flight by a factor $\lambda = 24\,000$, and consequently it is 24 000 times less sensitive to differential displacements. In order to demonstrate the feasibility of the space experiment to that level of sensitivity it should have detected relative displacements between the centers of mass of the test cylinders of $\lambda \cdot \Delta r_{\text{GG}} = 1.5 \cdot 10^{-2}$ μm , while so far we have achieved only 1.5 μm . In order to gain this factor of 100, so as to perform a better demonstration, we need to reduce the effects of the ground perturbations by the same amount. The significance of the ground demonstration improves by reducing the stiffness of the accelerometer (hence the scaling factor λ), together with a corresponding reduction of the effects of the ground perturbations. An improved version of the prototype currently under construction is designed to reach a scaling factor $\lambda = 2400$ and a stability in the relative displacements of the test cylinders of $1.5 \cdot 10^{-3}$ μm . By comparison with the target of the GG space experiment in testing the equivalence princi-

ple: $\eta_{\text{GG}} = \Delta a/a = 10^{-17}$ ($a = 840$ cm s^{-2} , $\Delta a = 8.4 \cdot 10^{-15}$ cm s^{-2}) this corresponds to a full scale test at the level $\eta_{\text{prototype}} = \lambda^2 \eta_{\text{GG}} = 5.8 \cdot 10^{-11}$, because $\Delta a = \omega_{\text{diff}}^2 \cdot \Delta r_{\text{GG}}$, the differential natural frequency ω_{diff} being proportional to the coupling stiffness of the suspensions.

The local acceleration of gravity, because of the need for a stiff suspension in the vertical direction, forces a few asymmetries in the design of the ground accelerometer which are not there in the instrument designed for space (as it is apparent by comparing Fig. 2 and Fig. 6) and reduce the advantages of the instrument for EP testing on the ground. Nevertheless, rotation (especially if at high rate)—and the corresponding frequency modulation of the signal—is extremely important, as the successful experiments by the “Eöt-Wash” group have demonstrated, in EP testing (Adelberger et al., 1990; Su et al., 1994; Baeßler et al., 1999) as well as in the measurement of the universal constant of gravity (Gundlach and Merkowitz, 2000) and in testing the inverse square law at sub-mm distances (Hoyle et al., 2001). Our accelerometer shows that fast rotation can be achieved, that it can be achieved with large test masses (which is very important to reduce thermal noise), that it is compatible with small force gravitation measurements and—most importantly—that is suitable for use in space. The dynamics of the system is understood, it can be theoretically anticipated and checked by the measurements. Losses measured with the full system in operation (and with mechanical suspensions of quite a complex shape; see Fig. 4), yield a quality factor only four times smaller than the value that is required for the GG space experiment to reach its target. As for the fact that the prototype can only check for violation in the field of the Sun and not of the Earth (because of the gyroscopic effects discussed in Section 2), it is worth stressing that also the best “Eöt-Wash” results have been obtained in the field of the Sun (Baeßler et al., 1999), in spite of the slightly weaker signal and the need for long term measurements in this case. The reason is the difficulty—when searching for an effect in a fixed direction—to model the spurious effects of local mass anomalies (the small ones nearby and the very large ones far away) which obviously do not rotate with the instrument. A difficulty which is totally eliminated in space where the whole spacecraft co-rotates with the test masses.

In summary, we can convincingly argue that theoretical understanding, numerical modeling and experimental measurements performed so far put on solid grounds the novel idea of a high accuracy space test of the equivalence principle (to one part in 10^{17}) with fast rotating weakly coupled test cylinders as proposed for the GG small mission. It has been shown (Nobili et al., 2001) that fast rotation and large mass of the test bodies are pivotal in making it possible to aim at such a high accuracy test in space with an experiment at room temperature. Among the proposed space experiments, GG is the only one in which the accelerometer devoted to EP testing and the one used for zero check (i.e., with test bodies made of the same material) are both centered at the center of mass of the spacecraft, so as to reduce common mode tidal effects and improve the reliability of the zero check. It is also the only one for which a full scale prototype of the accelerometer has been built and can be operated and tested on the ground.

Acknowledgements

This work is funded by the Italian national space agency (ASI), the national Ministry of University, Research and Technology (MURST) and the University of Pisa. Special thanks are due to the Italian space Industry LABEN (Divisione Proel Technologie, Firenze) for making available to us their laboratories and infrastructures.

Note added in proof

Recent work by Damour, Piazza and Veneziano (2002a, 2002b) suggests that the universality of free fall (hence the equivalence principle) might be violated near $\eta = \Delta a/a \sim 10^{-12}$. The prediction refers to pairs of test masses made of Cu and Be or Pt and Ti. The present experimental limit for Cu and Be is $\eta(\text{Be,Cu}) = (-1.9 \pm 2.5) \cdot 10^{-12}$ (Su et al., 1994). In Baeßler et al. (1999) the differential acceleration between test masses in the gravitational field of the Sun ($a_{\odot} \approx 0.6 \text{ cm s}^{-2}$) has a 1σ statistical uncertainty $\Delta a_{\odot} = 5.6 \cdot 10^{-13} \text{ cm s}^{-2}$, hence $\Delta a_{\odot}/a_{\odot} \sim 10^{-12}$. However, since this experiment compares accelerations of “earth’s core” and “moon/mantle” like test

bodies, the composition-dependent acceleration Δa_{CD} of the Earth and Moon towards the Sun is smaller than Δa_{\odot} because only a fraction of their mass is contained in their cores and mantles. The authors conclude that $\Delta a_{CD}/a_{\odot} = (+0.1 \pm 2.7 \pm 1.7) \cdot 10^{-13}$.

References

- Adelberger, E.G. et al., 1990. *PhRvD* 42, 3267.
 Baeßler, S. et al., 1999. *PhRvL* 83, 3585.
 Braginsky, V.B., Panov, V.I., 1972. *Sov. Phys. JEPT* 34, 463.
 Comandi, G., 1999. Laurea degree thesis in Physics (cum laude), University of Pisa available online <http://eotvos.dm.unipi.it/nobili/theses/comandi>
 Crandall, S.H., 1995. Rotordynamics. In: Kliemann, W., Namachchivaya, N.S. (Eds.), *Nonlinear Dynamics and Stochastic Mechanics*. CRC Press, Boca Raton, FL, pp. 1–44.
 Crandall, S.H., Nobili, A.M., 1997. On the Stabilization of the GG System available online <http://tycho.dm.unipi.it/nobili/ggweb/crandall>
 Damour, T., Piazza, F., Veneziano, G., 2002a. *PhRvL* 89, 081601.
 Damour, T., Piazza, F., Veneziano, G., 2002b. *PhRvD* 66, 046007.
 Den Hartog, J.P., 1985. *Mechanical Vibrations*. Dover, New York, first published 1934.
 Eötös, R.V., Pekar, D., Fekete, E., 1922. *Ann. Physik* 16, 11.
 “GALILEO GALILEI” (GG), Phase A Report, ASI (Agenzia Spaziale Italiana) (1998), 2nd Edition (2000) (<http://eotvos.dm.unipi.it/nobili/ggweb/phaseA>).
 “GALILEO GALILEI” (GG) Website: <http://eotvos.dm.unipi.it/nobili>
 Genta, G., 1993. *Vibration of Structures and Machines*. Springer, New York.
 Gundlach, J.H., Merkowitz, S.M., 2000. *PhRvL* 85, 2869.
 Hoyle, C.D. et al., 2001. *PhRvL* 86, 1418.
 Luo, J., 2000. Private communication.
 MICROSCOPE Website: http://www.cnes.fr/activites/activites/connaissance/physique/microsatellite/1sommaire_microsatellite.htm and <http://www.onera.fr/dmph-en/accelerometre>
 Nobili, A.M. et al., 1999. *Class. Quantum Grav.* 16, 1463.
 Nobili, A.M. et al., 2000. NASA Document D-18925, 309 (http://eotvos.dm.unipi.it/nobili/nasa_fp)
 Nobili, A.M. et al., 2001. *PhRvD* 63, 101101(R).
 Roll, P.G., Krotkov, R., Dicke, R.H., 1964. *Ann. Phys N.Y.* 26, 442.
 STEP Satellite Test of the Equivalence Principle, 1993. Report on the Phase A Study, ESA/NASA-SCI(93)4.
 STEP Satellite Test of the Equivalence Principle, 1996. Report on the Phase A Study, ESA-SCI(96)5.
 STEP Website: <http://einstein.stanford.edu/STEP>.
 Su, Y. et al., 1994. *PhRvD* 50, 3614.
 Touboul, P. et al., 2001. The Microscope mission, *Acta Astronautica*, in press.
 Worden, Jr. P.W., 1978. *Acta Astronautica* 5, 27.